Theory of the dispersive modulator

D. Grischkowsky* and M. M. T. Loy

IBM Thomas J. Watson Research Center, Yorktown Heights, New York 10598
(Received 28 October 1974)

The recent observations by Loy of amplitude modulation and compression of infrared laser pulses caused by passage through the dispersive modulator (a cell containing dilute NH_3 vapor with a Stark-modulated resonant frequency) are explained. It is shown that there is a formal equivalence between (i) the passage of a near-resonant light beam through a vapor with a time-dependent resonant frequency, and (ii) the passage of a frequency-modulated light beam through a vapor with a constant resonant frequency. For low-intensity light this equivalence reduces the problem to the optical analog of chirp radar.

PACS numbers: 42.80.K, 42.60.L

Most of the optical pulse compression methods demonstrated to date have been based on the idea of chirp radar,[1-3] where a frequency-modulated pulse is sent through a dispersive delay line. Recent work[3] has used light nearly resonant with an atomic transition and achieved strong pulse compression with a relatively small amount of frequency modulation. In this paper we consider a closely related system, Loy's dispersive modulator,[4] where instead of modulating the frequency of the light, the resonant frequency is modulated. There is a formal equivalence between these two methods, and we will show that the pulse reshaping is the same for both situations.

First, we will demonstrate the equivalence, and then calculate the pulse reshaping. We consider the electric field $\mathbf{E}$ to be represented by

$$\mathbf{E}(z,t)=\mathcal{E}(z,t)\hat{x}\cos[kz-\omega t-\phi(z,t)]. \tag{1}$$

Because the light is nearly resonant with an atomic transition, the propagation is very well described by the coupled reduced wave equations[5]

$$\frac{\partial\mathcal{E}}{\partial z}+\frac{1}{c}\frac{\partial\mathcal{E}}{\partial t}=-\frac{2\pi\omega}{c}v, \tag{2a}$$

$$\frac{\partial\phi}{\partial z}+\frac{1}{c}\frac{\partial\phi}{\partial t}=-\frac{2\pi\omega}{c\mathcal{E}}u, \tag{2b}$$

and the Bloch equations

$$\frac{\partial u}{\partial t}=v\Delta\omega'-\frac{u}{T_2}, \tag{3a}$$

$$\frac{\partial v}{\partial t}=-u\Delta\omega'-\frac{\kappa^2\mathcal{E}\hbar\Delta N}{2}-\frac{v}{T_2}, \tag{3b}$$

$$\frac{\partial\Delta N}{\partial t}=\frac{2\mathcal{E}v}{\hbar}. \tag{3c}$$

Here u and v are the in-phase and out-of-phase components of the polarization, respectively; $\Delta\omega'=\omega_0-\omega'$, where $\omega'=\omega+\partial\phi/\partial t$ is the instantaneous time-dependent frequency, and ω is the constant carrier frequency; T_2 is the homogeneous transverse relaxation time; $\kappa=\mu/\hbar$, where μ is the matrix element of the electric dipole moment between the two states; ΔN is the difference between the densities of atoms in the excited and ground states. For the parallel plate transmission line of Loy's experiment, the Stark voltage traveled at c to a very good approximation. Hence, the resonant frequency ω_0 was time dependent and also traveled at c, i.e.,

$$\frac{\partial\omega_0}{\partial z}+\frac{1}{c}\frac{\partial\omega_0}{\partial t}=0. \tag{4}$$

Taking the partial derivative with respect to time of Eq. (2b) and combining with Eq. (4), we obtain

$$\frac{\partial\Delta\omega'}{\partial z}+\frac{1}{c}\frac{\partial\Delta\omega'}{\partial t}=\frac{2\pi\omega}{c}\frac{\partial}{\partial t}\frac{u}{\mathcal{E}}. \tag{5}$$

Equations (2a), (3), and (5) show an important symmetry between a variation of the instantaneous frequency ω' and a variation of the resonant frequency ω_0.[6] Consequently, the output $\mathcal{E}(z,t)$ and $\Delta\omega'(z,t)$ depend only on the initial conditions $\mathcal{E}(0,t)$ and $\Delta\omega'(0,t)$. As long as $\Delta\omega'(0,t)$ is the same, $\mathcal{E}(z,t)$ and $\Delta\omega'(z,t)$ are independent of whether ω' or ω_0 or both are time dependent at $z=0$. The output intensity would be the same for these three cases, although the output frequency $\omega'(z,t)$ would be different.

Thus, when the intensity is low so that nonlinear polarization effects can be neglected, we can use chirp radar theory[1,2] (linear dispersion theory) to calculate the output intensity of the dispersive modulator: (i) the input beam is assumed to be frequency modulated and the resonant frequency ω_0 is assumed to be *constant*; (ii) the input light is Fourier analyzed; (iii) the Fourier components freely propagate through the dispersive delay line with their respective phase velocities; (iv) the output intensity is given by the square of the summation of the components at the end of the delay line. Following the above prescription, at $z=0$ the input to the dispersive modulator is considered to be

$$\mathbf{E}(0,t)=\mathcal{E}_0\hat{x}\cos(\omega t+\phi_0\sin\Lambda t), \tag{6}$$

where $\mathcal{E}_0$ is a constant, ϕ_0 is the amplitude of the equivalent phase modulation, and Λ is the angular modulation frequency. Equation (6) is the same as[7]

$$\mathbf{E}(0,t)=\mathcal{E}_0\hat{x}\Big(J_0(\phi_0)\cos\omega t+\sum_{j=1}^{\infty}J_j(\phi_0)[\cos(\omega+j\Lambda)t+(-1)^j\cos(\omega-j\Lambda)t]\Big), \tag{7}$$

with $J_j(\phi_0)$ designating the Bessel function of order j with argument ϕ_0. The output field is then given by the

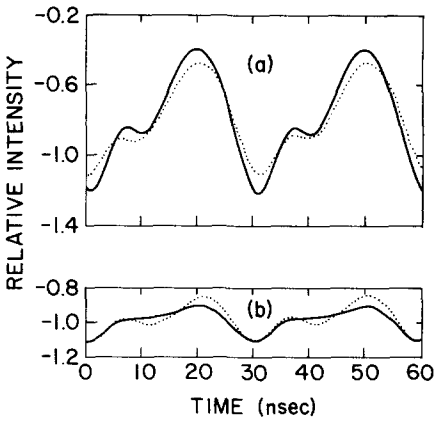

FIG. 1. Comparison between theory (solid line) and experiment (dotted line) for the output of the dispersive modulator. (a) Experimental results from Fig. 2(b) of Ref. 4. (b) Experimental results from Fig. 2(c) of Ref. 4.

sum of the Fourier components at the end of the delay line of length z:

$$\mathbf{E}(z,t)=\mathcal{E}_0\hat{x}\Big(\exp[-(\alpha_0 z/2)]\,J_0(\phi_0)\cos(k_0 z-\omega t) + \sum_{j=1}^{\infty} J_j(\phi_0)\{\exp[-(\alpha_j^{+}z/2)]\cos[k_j^{+}z-(\omega+j\Lambda)t] + (-1)^j\exp[-(\alpha_j^{-}z/2)]\cos[k_j^{-}z-(\omega-j\Lambda)t]\}\Big). \quad (8)$$

In Eq. (8) α_0, α_j^{+}, and α_j^{-} are the absorption coefficients for light with angular frequencies ω, $(\omega+j\Lambda)$, and $(\omega-j\Lambda)$, respectively; similarly, k_0, k_j^{+}, and k_j^{-} are the propagation vectors.

For a Doppler-broadened line, whose homogeneous linewidth is much smaller than the Doppler width $\Delta\omega_D$ (FWHM), the absorption coefficient $\alpha(\omega)$ at frequency ω is given by

$$\alpha(\omega)=[16\pi^3 N\mu^2(\ln 2/\pi)^{1/2}/(\lambda\hbar\Delta\omega_D)] \times\exp\{-[(2\Delta\omega/\Delta\omega_D)^2\ln 2]\}. \quad (9)$$

N is the number density, and $\Delta\omega=\omega_0-\omega$. Similarly, the index of refraction n is given by

$$n(\omega)=1+\frac{4\pi N\mu^2(\ln 2)^{1/2}}{\hbar\Delta\omega_D}P\int_{-\infty}^{+\infty}\frac{\exp(-t^2)\,dt}{(t-x)\pi^{1/2}}, \quad (10)$$

with $x=-(\ln 2)^{1/2}\,2\Delta\omega/\Delta\omega_D$. P indicates the principal value of the integral, the plasma dispersion function.[8] For large x, Eq. (10) reduces to $n(\omega)$ for a single resonance line.[5]

Figure 1 is a comparison of the calculated output (solid curves) from the dispersive modulator with the experimental results (dotted curves) of Figs. 2(b) and 2(c) of Ref. 4. All the parameters in the calculation were experimentally measured. However, the low-intensity absorption coefficients α_j given by Eq. (9) were reduced when saturation (hole-burning) effects were important. For the experimental conditions of Fig. 2(a) of Ref. 4, this complicated the physical situation so much that we could not make a meaningful comparison with theory. For Fig. 2(b) of Ref. 4, saturation effects were partially accounted for by simply multiplying all the calculated α_j by 0.4. For all the other cases, the low-intensity α_j given by Eq. (9) were used. The dispersion curve is little changed by hole burning, and the use of Eq. (10) is reasonably accurate in all cases. The input intensity was normalized to unity for all the calculations. Experimentally, fluctuations in the input power of approximately ± 10% led to an uncertainty in the normalized output by this amount. For the relatively small argument ϕ_0 of the Bessel functions the calculation was terminated at $j=6$.

Figure 2 shows the calculated output for the experimental conditions of Fig. 3 of Ref. 4. Here, ϕ_0 was relatively large, and the calculation was carried out to $j=18$. Due to the relatively large frequency offset of 500 MHz, absorption had little effect in determining the output pulse shape. The relative magnitude of the reshaping as a function of the modulation strength is in good agreement with experiment. Also, the calculated duration of the output spikes agrees well with the observations. The absence of high-frequency ringing in the experimental results is probably due to the slow detector rise time of approximately 3 nsec. However, the ringing can be eliminated by operating the modulator under different conditions, such as those for the theoretically equivalent case of Ref. 3.

The authors would like to acknowledge useful discussions with J.A. Armstrong and J.J. Wynne, and the skilled technical assistance of R.J. Bennett.

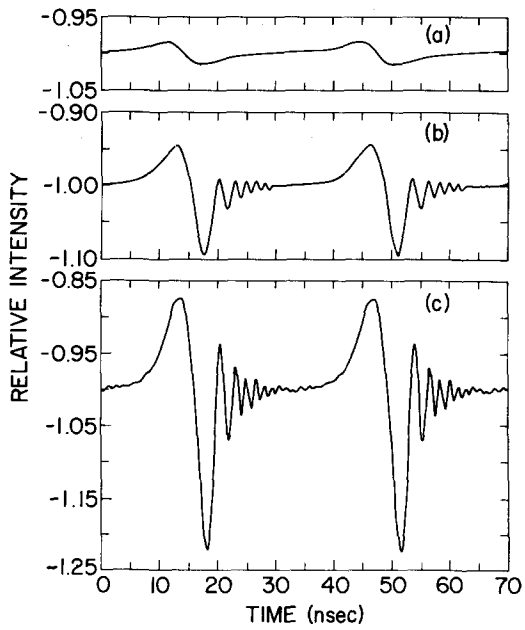

FIG. 2. Calculated output of the dispersive modulator as a function of modulation strength for the experimental conditions of Fig. 3 of Ref. 4.

*Work partially supported by the Office of Naval Research.
[1]J.R. Klauder, A.C. Price, S. Darlington, and W.J. Albersheim, Bell Syst. Tech. J. **39**, 745 (1960).
[2]J.A. Giordmaine, M.A. Duguay, and J.W. Hansen, IEEE J. Quantum Electron. **QE-4**, 252 (1968).
[3]D. Grischkowsky, Appl. Phys. Lett. **25**, 566 (1974).
[4]M.M.T. Loy, Appl. Phys. Lett. **26**, 98 (1975).
[5]D. Grischkowsky, in *Laser Applications to Optics and Spectroscopy*, Vol. II of *Physics of Quantum Electronics Series*, edited by S.F. Jacobs, M. Sargent III, and M.O. Scully (Addison-Wesley, Reading, Mass., 1974).
[6]C.H. Townes and A.L. Schawlow, *Microwave Spectroscopy* (McGraw-Hill, New York, 1955), p. 278. Here, this symmetry is noted in an absorption calculation for a modulated resonant frequency.
[7]August Hund, *Frequency Modulation* (McGraw-Hill, New York, 1942), p. 350.
[8]B.D. Fried and S.D. Conte, *The Plasma Dispersion Function* (Academic, New York, 1961).

Porous-wall BeO capillary waveguide laser

A. Papayoanou and A. Fujisawa*

United States Army Electronics Command, Fort Monmouth, New Jersey 07703
(Received 6 November 1974)

Small-bore capillary tubes exhibit very high optical gains and saturation intensities in flowing gas CO_2 systems. However, these parameters may vary greatly in the axial direction due to the nonuniform axial pressure distribution. Use of porous-wall BeO capillary tubes makes it possible to attain a more uniform pressure distribution and to usefully scale capillary waveguide amplifiers to longer lengths.

PACS numbers: 42.60.L, 42.50.

Earlier research has established that the waveguide capillary laser has very high optical gain and saturation intensity in flowing CO_2 systems.[1-3] However, it has been noted, at least for 1-mm bore tubes, that the gain per unit length decreased strongly as the tube length was increased.[1,2] Such a limitation ultimately establishes a limit in scaling such tubes to longer lengths.

The reason for the decreased gain per unit length as the tube length is increased is presumably due to the nonuniform axial pressure distribution occurring in longitudinal flow. It should be remembered that for typical capillary flow conditions a Hagen-Poiseuille flow is established and is sustained by a pressure gradient in the direction of flow. Hence, the pressure decreases linearly along the tube axis from some high input pressure P_1 to some lower exit pressure P_0. The equation for such flow can be put into the form[4]

$$F=\frac{\pi a^4}{4\eta}\frac{P_1+P_0}{2kT}\frac{P_1-P_0}{l}, \tag{1}$$

where F is the number of gas molecules flowing per unit time through the capillary of length l, η is the gas viscosity, a is the bore radius, k is the Boltzmann constant, and T is the absolute gas temperature. Thus, the gas flow in the tube depends on the tube dimensions a and l as well as the pressure differential. For some flow speed which optimizes the gain, a certain pressure differential is required. It was found that for CO_2 mixtures pressure ratios P_1/P_0 of about 5 were required to attain optimum flow rates in 1-mm-bore 10.2-cm-long tubes.[2] For longer tubes this ratio would increase proportionately leading to highly variable gain and saturation intensities along the tube axis.

To reduce this axial pressure inhomogeneity we have used a porous-wall 1-mm-bore BeO capillary tube which allows the gas to be introduced into the discharge volume with greater axial uniformity. The gas enters the central bore through the pores from a high-pressure chamber (0.1–1 atm depending on capillary tube pressures and flow conditions) surrounding the tube as shown in Fig. 1. A pump pulls the gas out both ends of the tube. Tube wall temperature was monitored with a thermistor probe mounted on the tube wall. The thermal conductivity of the porous-wall BeO tubes used was experimentally determined to be 5–6 times lower than that of dense BeO. This necessitated cooling the tube along its length to prevent large longitudinal temperature rises. A copper cooling block, 10 cm long, contoured to the tube outer radius was placed in contact with the tube over an azimuth of 120° for this purpose. Despite the reduced thermal conductivity, the radial temperature rise from the outer to the inner wall was calculated, for operative power input levels, to be only

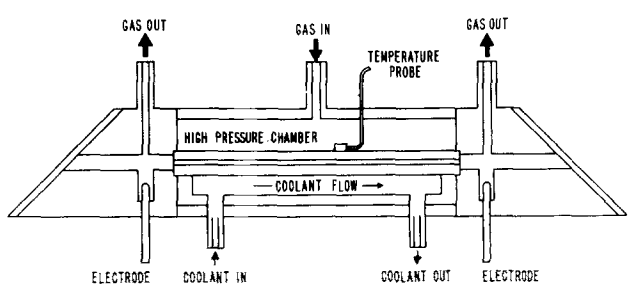

FIG. 1. Amplifier setup used. Porous-wall BeO tube is shown in center of high-pressure chamber. Tube length was 12.5 cm and bore diameter was 1 mm.

